

Spin susceptibility and fluctuation corrections in the BCS-BEC crossover regime of an ultracold Fermi gas

Takashi Kashimura, Ryota Watanabe, and Yoji Ohashi

Department of Physics, Keio University,

3-14-1 Hiyoshi, Kohoku-ku, Yokohama 223-8522, Japan

(Dated: June 2, 2022)

Abstract

We investigate magnetic properties and effects of pairing fluctuations in the BCS (Bardeen-Cooper-Schrieffer)-BEC (Bose-Einstein condensation) crossover regime of an ultracold Fermi gas. Recently, Liu and Hu, and Parish, pointed out that the strong-coupling theory developed by Nozières and Schmitt-Rink (NSR), which has been extensively used to successfully clarify various physical properties of cold Fermi gases, unphysically gives *negative* spin susceptibility in the BCS-BEC crossover region. The same problem is found to also exist in the ordinary non-self-consistent T -matrix approximation. In this paper, we clarify that this serious problem comes from incomplete treatment in term of pseudogap phenomena originating from strong pairing fluctuations, as well as effects of spin fluctuations on the spin susceptibility. Including these two key issues, we construct an extended T -matrix theory which can overcome this problem. The resulting *positive* spin susceptibility agrees well with the recent experiment on a ${}^6\text{Li}$ Fermi gas done by Sanner and co-workers. We also apply our theory to a polarized Fermi gas to examine the superfluid phase transition temperature T_c , as a function of the polarization rate. Since the spin susceptibility is an important physical quantity, especially in singlet Fermi superfluids, our results would be useful in considering how singlet pairs appear above and below T_c in the BCS-BEC crossover regime of cold Fermi gases.

PACS numbers: 03.75.Ss, 03.75.-b, 03.70.+k

I. INTRODUCTION

The uniform spin susceptibility χ is a fundamental quantity in considering magnetic properties of an electron system. In a free electron gas, χ gives useful information about the single-particle density of states at the Fermi level [1]. In *s*-wave superconductivity, χ is suppressed below the superconducting phase transition temperature T_c to vanish at $T = 0$ [2], because the spin degrees of freedom become inactive by the formation of singlet Cooper pairs. The suppression of the spin susceptibility has been also observed in the underdoped regime of high- T_c cuprates, which is referred to as the spin gap phenomenon in the literature [3]. Although the origin of the spin gap is still in debate, the importance of preformed pairs has been pointed out [4].

Since the realization of superfluid ^{40}K [5] and ^6Li [6–8] Fermi gases, the high tunability of this quantum system has attracted much attention [9–11]. Indeed, using a tunable pairing interaction associated with a Feshbach resonance [12], one can study superfluid properties from the weak-coupling BCS regime to the strong-coupling BEC limit in a unified manner (BCS-BEC crossover) [13–17]. In the so-called crossover region, a deviation of single-particle excitation spectrum from the free particle dispersion has been observed in the normal state, by using the photoemission-type experiment developed by JILA group [18, 19]. As an explanation for this anomaly, the possibility of the pseudogap phenomenon associated with strong pairing fluctuations has been proposed [20–27]. Since the cold Fermi gas system is much simpler than high- T_c cuprates, the former system would be useful for the assessment of the preformed-pair scenario discussed in the latter.

Besides the tunable interaction, the high tunability of population imbalance is another advantage of cold Fermi gases [28, 29]. When we describe two atomic hyperfine states in a Fermi gas by pseudospin $\sigma = \uparrow, \downarrow$, a polarized Fermi gas is closely related to an electron system under an external magnetic field. In the limit of low population imbalance, one may evaluate the spin susceptibility. Using this quantity, one can examine whether the preformed singlet pairs really appear in the BCS-BEC crossover regime of a cold Fermi gas. In the case of a finite population imbalance, the mismatch of the Fermi surfaces between the \uparrow -spin component and \downarrow -spin component is expected to cause the instability of the *s*-wave superfluid state [30], where various exotic states have been proposed, such as the Fulde-Ferrel-Larkin-Ovchinnikov (FFLO) state [31, 32] and the Sarma phase [33–35].

In this paper, we investigate (pseudo)magnetic properties of a normal state Fermi gas in the BCS-BEC crossover region. In the unpolarized case, the strong-coupling theory developed by Nozières and Schmitt-Rink (NSR) [15] has been extensively used to successfully clarify various physical properties of this system [17, 20, 21, 23, 26, 36–41]. However, when we apply this theory to a polarized Fermi gas, it is known that negative spin susceptibility is obtained in the crossover region [42, 43] (which is thermodynamically forbidden [44]). Because of this serious problem, so far, the phase diagram of a polarized Fermi gas has mainly been examined within the mean-field level [35]. However, as in the unpolarized case, strong-coupling effects would be also important in the BCS-BEC crossover regime of a polarized Fermi gas. Indeed, it has been pointed out that the FFLO state (which has been predicted in a polarized Fermi gas within the mean-field analysis [35]) is unstable against pairing fluctuations [45, 46]. Thus, to discuss the BCS-BEC crossover physics of a polarized Fermi gas, we need a reliable and tractable strong-coupling theory which can overcome the above mentioned problem.

In this paper, we show that the “negative susceptibility problem” also exists in the ordinary (non-self-consistent) T -matrix approximation, which has been also extensively used in the unpolarized case. Clarifying the origin of this serious problem, we present a minimal extension of the T -matrix theory to correctly give the required positive spin susceptibility in the whole BCS-BEC crossover region. The calculated spin susceptibility in this extended T -matrix theory is shown to agree well with the recent experiment on a ${}^6\text{Li}$ Fermi gas [47]. We also apply this theory to the system with finite population imbalance, and examine the critical population imbalance at which the superfluid phase transition disappears.

This paper is organized as follows. In Sec.II, we explain our formulation. We also compare our theory with the NSR theory, as well as the ordinary T -matrix approximation. In Sec.III, we calculate the spin susceptibility to show that our strong-coupling theory does not meet the negative susceptibility problem in the whole BCS-BEC crossover region. We also compare our results with the recent experiment on a ${}^6\text{Li}$ Fermi gas. In Sec.IV, we treat a polarized Fermi gas. Throughout this paper, we set $\hbar = k_B = 1$, and the system volume V is taken to be unity.

II. MODEL POLARIZED FERMI GAS AND STRONG-COUPLING THEORIES

We consider a two-component Fermi gas with population imbalance, described by the BCS Hamiltonian,

$$H = \sum_{\mathbf{p},\sigma} \xi_{\mathbf{p},\sigma} c_{\mathbf{p},\sigma}^\dagger c_{\mathbf{p},\sigma} - U \sum_{\mathbf{p},\mathbf{p}',\mathbf{q}} c_{\mathbf{p}+\mathbf{q}/2,\uparrow}^\dagger c_{-\mathbf{p}+\mathbf{q}/2,\downarrow}^\dagger c_{-\mathbf{p}'+\mathbf{q}/2,\downarrow} c_{\mathbf{p}'+\mathbf{q}/2,\uparrow}. \quad (1)$$

Here, $c_{\mathbf{p},\sigma}^\dagger$ is the creation operator of a Fermi atom with momentum \mathbf{p} and pseudospin $\sigma = \uparrow, \downarrow$, describing two atomic hyperfine states. $\xi_{\mathbf{p},\sigma} = \varepsilon_{\mathbf{p}} - \mu_\sigma = \frac{p^2}{2m} - \mu_\sigma$ is the kinetic energy of the σ -spin component, measured from the Fermi chemical potential μ_σ (where m is an atomic mass). The pairing interaction $-U$ (< 0) is assumed to be tunable by a Feshbach resonance. As usual, we measure the interaction strength in terms of the s -wave scattering length a_s , given by

$$\frac{4\pi a_s}{m} = \frac{-U}{1 - U \sum_{\mathbf{p}}^{\omega_c} \frac{1}{2\varepsilon_{\mathbf{p}}}}, \quad (2)$$

where ω_c is a high-energy cutoff. In this scale, the weak-coupling BCS regime and the strong-coupling BEC regime are characterized by $(k_F a_s)^{-1} \lesssim -1$ and $(k_F a_s)^{-1} \gtrsim 1$, respectively. (Here, $k_F = [3\pi^2 N]^{1/3}$ is the Fermi momentum, where N is the total number of Fermi atoms.) The region $-1 \lesssim (k_F a_s)^{-1} \lesssim 1$ is called the crossover region. In this paper, we consider a uniform Fermi gas, for simplicity.

When we write the chemical potential μ_σ as $\mu_\sigma = \mu + \sigma h$ [where $\mu = (\mu_\uparrow + \mu_\downarrow)/2$ is the averaged chemical potential], Eq. (1) may be viewed as a model Hamiltonian for an interacting electron system under an external magnetic field h . The spin susceptibility χ is then given by

$$\chi = \lim_{h \rightarrow 0} \frac{N_\uparrow - N_\downarrow}{h}. \quad (3)$$

Here, N_σ is the number of Fermi atoms with σ -spin, which is calculated from the single-particle thermal Green's function $G_{\mathbf{p},\sigma}(i\omega_n)$ as

$$N_\sigma = T \sum_{\mathbf{p}, i\omega_n} G_{\mathbf{p},\sigma}(i\omega_n), \quad (4)$$

where ω_n is the fermion Matsubara frequency. In this formalism, strong-coupling effects on χ is described by the self-energy $\Sigma_{\mathbf{p},\sigma}(i\omega_n)$ in $G_{\mathbf{p},\sigma}(i\omega_n)$,

$$G_{\mathbf{p},\sigma}(i\omega_n) = \frac{1}{[G_{\mathbf{p},\sigma}^0(i\omega_n)]^{-1} - \Sigma_{\mathbf{p},\sigma}(i\omega_n)}. \quad (5)$$

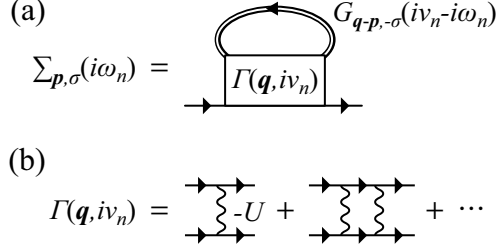


FIG. 1: (a) Self-energy $\Sigma_{\mathbf{p},\sigma}(i\omega_n)$ used in this paper. (b) Particle-particle vertex function $\Gamma(\mathbf{q}, i\nu_n)$. The solid line and the solid double line represent the free Green's function G^0 and the full Green's function G in Eq. (5), respectively. The wavy line describes the attractive interaction $-U$.

Here, $G_{\mathbf{p},\sigma}^0(i\omega_n) = [i\omega_n - \xi_{\mathbf{p},\sigma}]^{-1}$ is the Green's function for a free Fermi gas.

As mentioned in the introduction, the NSR theory breaks down for a polarized Fermi gas in the sense that it incorrectly gives the negative spin susceptibility ($\chi < 0$) in the BCS-BEC crossover region [42, 43]. This implies that one needs to carefully treat the self-energy correction $\Sigma_{\mathbf{p},\sigma}(i\omega_n)$ in considering magnetic properties of a polarized Fermi gas. In this paper, we take the strong-coupling corrections diagrammatically described by Fig.1 (We will explain the reason for this choice in Sec.III.), which gives

$$\Sigma_{\mathbf{p},\sigma}(i\omega_n) = T \sum_{\mathbf{q}, i\nu_n} \Gamma(\mathbf{q}, i\nu_n) G_{\mathbf{q}-\mathbf{p},-\sigma}(i\nu_n - i\omega_n), \quad (6)$$

where ν_n is the boson Matsubara frequency. $\Gamma(\mathbf{q}, i\nu_n)$ is the particle-particle vertex function in the ladder approximation (See Fig.1(b).),

$$\Gamma(\mathbf{q}, i\nu_n) = \frac{-U}{1 - U\Pi(\mathbf{q}, i\nu_n)}, \quad (7)$$

where

$$\begin{aligned} \Pi(\mathbf{q}, i\nu_n) &= T \sum_{\mathbf{p}, i\omega_n} G_{\mathbf{p}+\mathbf{q}/2,\uparrow}^0(i\nu_n + i\omega_n) G_{-\mathbf{p}+\mathbf{q}/2,\downarrow}^0(-i\omega_n) \\ &= - \sum_{\mathbf{p}} \frac{1 - f(\xi_{\mathbf{p}+\mathbf{q}/2,\uparrow}) - f(\xi_{-\mathbf{p}+\mathbf{q}/2,\downarrow})}{i\nu_n - \xi_{\mathbf{p}+\mathbf{q}/2,\uparrow} - \xi_{-\mathbf{p}+\mathbf{q}/2,\downarrow}} \end{aligned} \quad (8)$$

is the lowest order pair propagator. In Eq. (8), $f(x)$ is the Fermi distribution function.

The ordinary (non-self-consistent) T -matrix approximation (TMA) also uses the self-energy in Fig.1, except that the full Green's function G in Fig.1(a) is replaced by the

noninteracting one G^0 , as

$$\Sigma_{\mathbf{p},\sigma}^0(i\omega_n) = T \sum_{\mathbf{q},i\nu_n} \Gamma(\mathbf{q}, i\nu_n) G_{\mathbf{q}-\mathbf{p},-\sigma}^0(i\nu_n - i\omega_n). \quad (9)$$

In this sense, our strong-coupling theory may be regarded as an extended T -matrix approximation (ETMA) [48]. We briefly note that, although the NSR theory also uses $\Sigma_{\mathbf{p},\sigma}^0(i\omega_n)$, the Green's function in Eq. (5) is expanded to $O(\Sigma^0)$ as

$$G_{\mathbf{p},\sigma}^{\text{NSR}}(i\omega_n) = G_{\mathbf{p},\sigma}^0(i\omega_n) + G_{\mathbf{p},\sigma}^0(i\omega_n) \Sigma_{\mathbf{p},\sigma}^0(i\omega_n) G_{\mathbf{p},\sigma}^0(i\omega_n). \quad (10)$$

As usual, the superfluid phase transition temperature T_c is determined from the Thouless criterion,

$$\Gamma^{-1}(\mathbf{q}, i\nu_n = 0) \Big|_{T=T_c} = 0. \quad (11)$$

While the uniform superfluid state corresponds to $\mathbf{q} = 0$, the FFLO state is realized when the highest T_c is obtained at $\mathbf{q} \neq 0$. However, since the latter is known to be unstable against pairing fluctuations even for a weak interaction in the absence of a optical lattice [45, 46], we set $\mathbf{q} = \mathbf{0}$ in Eq. (11) from the beginning. In this case, the (regularized) T_c -equation is given by

$$\frac{m}{4\pi a_s} + \sum_{\mathbf{p}} \left\{ \frac{1}{4\xi_{\mathbf{p}}} \left[\tanh\left(\frac{\xi_{\mathbf{p},\uparrow}}{2T}\right) + \tanh\left(\frac{\xi_{\mathbf{p},\downarrow}}{2T}\right) \right] - \frac{1}{2\epsilon_{\mathbf{p}}} \right\} = 0, \quad (12)$$

where $\xi_{\mathbf{p}} = \epsilon_{\mathbf{p}} - \mu$ is the kinetic energy, measured from the averaged chemical potential $\mu = (\mu_{\uparrow} + \mu_{\downarrow})/2$. For a given total number of Fermi atoms $N = N_{\uparrow} + N_{\downarrow}$, we solve Eq. (12), together with the number equation (4), to determine T_c , μ , and h , self-consistently. In the unpolarized case, the three strong-coupling theories (ETMA, TMA, and NSR) qualitatively give the same BCS-BEC crossover behavior of T_c , as shown in Fig.2. In the next section, however, we show that they give very different results for the spin susceptibility.

III. SPIN SUSCEPTIBILITY IN THE BCS-BEC CROSSOVER REGION

Figure 3 shows the spin susceptibility χ at T_c in the BCS-BEC crossover. As mentioned previously, the NSR theory gives the negative spin susceptibility ($\chi_{\text{NSR}} < 0$), when the interaction becomes strong to some extent. The situation becomes better in the ordinary T -matrix theory (χ_{TMA}). However, as shown in the inset of Fig.3, χ_{TMA} slightly becomes

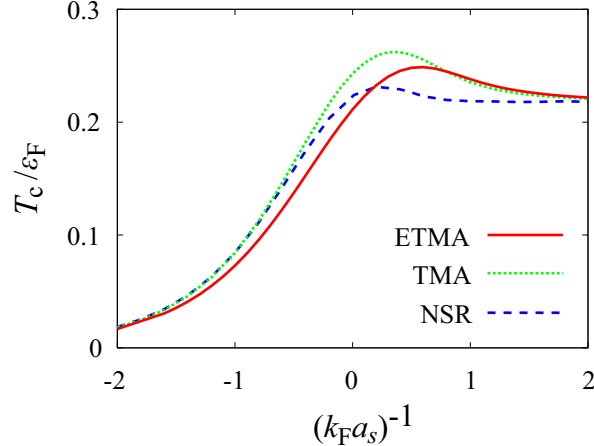


FIG. 2: (color online) Calculated T_c of an unpolarized Fermi gas in the extended T -matrix approximation (ETMA). For comparison, we also show the results in the ordinary T -matrix approximation (TMA), as well as the NSR theory (NSR). The interaction strength is measured in terms of the inverse scattering length a_s , normalized by the Fermi momentum k_F . ϵ_F is the Fermi energy.

negative in the crossover region. In contrast, our extended T -matrix approximation (χ_{ETMA}) gives the required *positive* spin susceptibility in the whole BCS-BEC crossover. χ_{ETMA} decreases with increasing the interaction strength, which reflects the increase of preformed Cooper pairs at T_c . Since all the Fermi atoms form tightly bound singlet molecules in the BEC limit, χ_{ETMA} vanishes in this limit.

To understand the reason why the present ETMA can overcome the negative susceptibility problem, it is helpful to note that strong-coupling effects on χ can be divided into the self-energy part and the vertex part, as diagrammatically shown in Fig.4(a). Between the two, the former comes from the self-energy correction $\Sigma_{\mathbf{p},\sigma}(i\omega_n)$ in the single-particle Green's function in Eq. (5), so that this part physically describes how strong-coupling effects on single-particle excitations affect the spin susceptibility χ . In this regard, we recall that strong-pairing fluctuations cause the pseudogap phenomenon in the crossover region [20–27], where a gap-like structure appears in the normal state density of states $\rho(\omega)$ around the Fermi level $\omega = 0$. Since χ is deeply related to $\rho(0)$ [1, 49], the pseudogap leads to the suppression of χ in the crossover region.

However, as pointed out in Ref. [20], the NSR theory overestimates the pseudogap to incorrectly give the *negative* density of states around $\omega = 0$. This is because of the fact

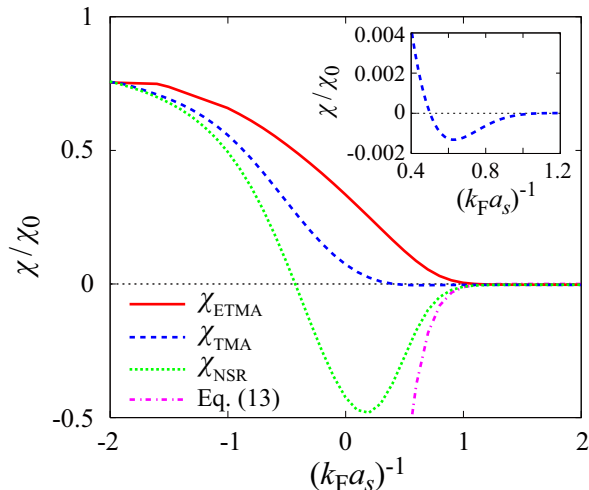


FIG. 3: (color online) Calculated spin susceptibility χ at T_c in the BCS-BEC crossover. χ_{ETMA} : extended T -matrix approximation. χ_{TMA} : ordinary T -matrix approximation. χ_{NSR} : NSR theory. The asymptotic form of χ_{NSR} in Eq. (13) in the NSR theory is also shown. The inset shows χ_{TMA} magnified in the crossover region where it becomes negative. χ_0 is the spin susceptibility of a free Fermi gas at $T = 0$.

that the NSR theory only retains the self-energy correction to $O(\Sigma^0)$. Thus, the NSR spin susceptibility χ_{NSR} also becomes negative in the crossover region where the pseudogap becomes remarkable in $\rho(\omega)$. Using the NSR Green's function in Eq. (10), one finds that χ_{NSR} is diagrammatically given by Fig.4(b). In this panel, the second term ($\equiv \chi_{\text{NSR}}^{(\text{b2})}$) describes the pseudogap correction to χ [50], which becomes dominant over the third term (which describes a vertex correction) in the BEC regime. In the BEC limit, one finds

$$\begin{aligned} \chi_{\text{NSR}}^{\text{BEC}} &\simeq \bar{\chi}_0 + \chi_{\text{NSR}}^{(\text{b2})} \\ &= \bar{\chi}_0 - \frac{16\pi a_s}{m} \left(\frac{2mT_c^{\text{BEC}}}{2\pi} \right)^{\frac{3}{2}} \zeta \left(\frac{3}{2} \right) \frac{\partial^2 N_{\uparrow}^0}{\partial h^2} \Big|_{h=0}. \end{aligned} \quad (13)$$

(We summarize the derivation in Appendix A.) Here,

$$\bar{\chi}_0 = \frac{1}{2T} \sum_{\mathbf{p}} \text{sech}^2 \left(\frac{\xi_{\mathbf{p}}}{2T} \right) \quad (14)$$

is the spin susceptibility of a non-interacting Fermi gas. In Eq. (13), $N_{\uparrow}^0 = \sum_{\mathbf{p}} f(\xi_{\mathbf{p},\uparrow})$ is the number of \uparrow -spin atoms in a free Fermi gas. $T_c^{\text{BEC}} = 0.218\varepsilon_{\text{F}}$ is T_c in the BEC limit [15–17]. Since the non-interacting part $\bar{\chi}_0$ in Eq. (13) is remarkably suppressed in the BEC regime

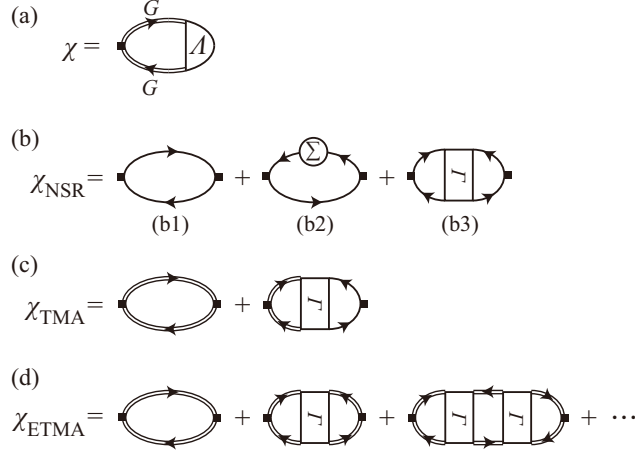


FIG. 4: (a) Feynman diagram describing spin susceptibility χ . The solid double line is the full Green's function involving the self-energy correction. Λ is a three-point vertex part. (b) χ_{NSR} . We only retain the terms to $O(\Sigma^0)$. (c) χ_{TMA} . (d) χ_{ETMA} . In panels (b)-(d), Γ is the particle-particle scattering matrix in the ladder approximation in Fig.1(b).

due to the negative chemical potential ($\mu < 0$) [14–17], the correction term $\chi_{\text{NSR}}^{(b2)}$ leads to the negative spin susceptibility, as shown in Fig. 3.

The pseudogap effect on $\rho(\omega \sim 0)$ is correctly treated in TMA [20–27]. However, this approximation still has a problem in the vertex part Λ , so that χ_{TMA} becomes negative in the crossover region. To see the origin of this, we diagrammatically compare χ_{TMA} (where the self-energy Σ^0 in Eq. (9) is used) with χ_{ETMA} (where the self-energy Σ in Eq. (6) is used) in Fig.4. While χ_{ETMA} involves the random phase approximation (RPA)-like series of the Maki-Thompson (MT) diagrams [50, 51], TMA only retains this series to the first order. When we approximate the particle-particle scattering matrix Γ to the bare interaction $-U$, and ignore all the other interaction effects, χ_{ETMA} in Fig.4(d) reduces to the RPA susceptibility,

$$\chi_{\text{ETMA}} \simeq \frac{\bar{\chi}_0}{1 + U\bar{\chi}_0}. \quad (15)$$

That is, the vertex part $\Lambda_{\text{ETMA}} \equiv 1/[1 + U\bar{\chi}_0]$, as well as χ_{ETMA} , are always positive. In contrast, because of

$$\chi_{\text{TMA}} \simeq \bar{\chi}_0[1 - U\bar{\chi}_0], \quad (16)$$

χ_{TMA} becomes negative, when the vertex part $\Lambda_{\text{TMA}} \equiv 1 - U\bar{\chi}_0$ becomes negative [52].

Since the present ETMA correctly treats both the self-energy part and the vertex part, the

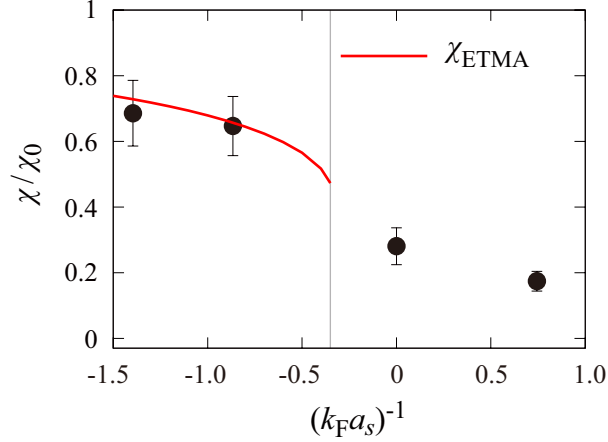


FIG. 5: (color online) Calculated spin susceptibility χ in the normal state (solid line). The experimental data [47] are shown as the solid circles. To reproduce the experimental situation [47], the temperature is fixed at the value of T_c for $(k_F a_s)^{-1} = -0.35$ (vertical line). While the left side of the vertical line is the normal phase, the right side is the superfluid phase.

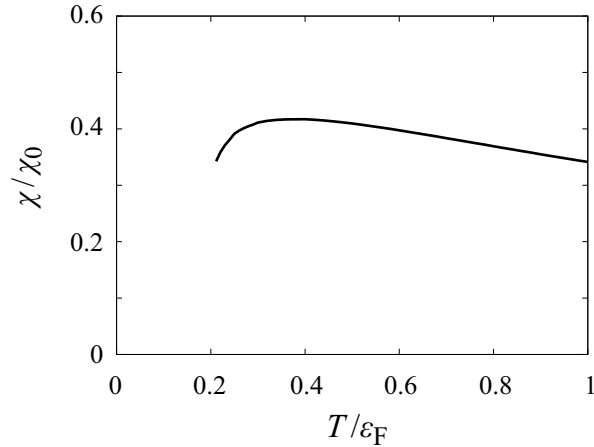


FIG. 6: Calculated spin susceptibility χ in the normal state above T_c . We take $(k_F a_s)^{-1} = 0$. Near T_c , the decrease of χ with decreasing the temperature is due to the pseudogap effect.

required positive spin susceptibility is obtained over the entire BCS-BEC crossover region, as shown in Fig.3.

In Fig. 5, we compare the calculated spin susceptibility χ_{ETMA} with the recent experiment on a ${}^6\text{Li}$ Fermi gas [47]. In this experiment, the temperature is fixed at the value of T_c for $(k_F a_s)^{-1} = -0.35$, and the spin susceptibility is measured from the *in situ* imaging of

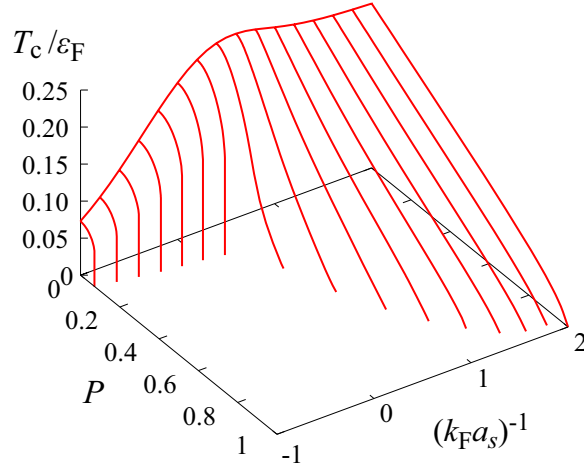


FIG. 7: (color online) Calculated T_c , as a function of the interaction strength and the polarization rate $P = [N_\uparrow - N_\downarrow]/[N_\uparrow + N_\downarrow]$. In this figure, we assume the second-order phase transition [57].

dispersive speckle patterns. In the normal state above T_c (the left side of the vertical line in Fig.5), χ_{ETMA} agrees well with the observed spin susceptibility, without introducing any fitting parameter.

While a good agreement with Ref. [47] is obtained, our result is somehow different from the experimental result done by Sommer and co-workers [53]. In this experiment, the observed spin susceptibility in the normal state monotonically increases with decreasing the temperature. In contrast, the calculated spin susceptibility exhibits a peak structure, as shown in Fig. 6. This non-monotonic behavior is similar to the so-called spin gap phenomenon observed in the underdoped regime of high- T_c cuprates [54]. In the present case, the decrease of χ near T_c is due to the development of the pseudogap in the single-particle density of states. For this discrepancy between the theory and experiment [53], although further analyses would be necessary, we note that Refs. [55, 56] have recently pointed out that the experimental result may be understood by taking into account the non-equilibrium state associated with a quasi-repulsive interaction.

IV. POLARIZED FERMI GAS IN THE BCS-BEC CROSSOVER REGIME

We now consider the case of finite population imbalance. Figure 7 shows T_c in the BCS-BEC crossover regime of a polarized Fermi gas ($N_\uparrow > N_\downarrow$), calculated within the framework

of ETMA. We briefly note that, since we are using the Thouless criterion in Eq. (12), the second-order phase transition is implicitly assumed. That is, possibility of the phase separation, which is accompanied by the first-order phase transition, is ignored in this figure.

In the strong-coupling BEC limit, the system is well described by a mixture of N_{\downarrow} tightly bound molecular bosons and $N_{\uparrow} - N_{\downarrow}$ excess \uparrow -spin atoms. Thus, the superfluid phase transition is dominated by the BEC of the former component. Since the phase transition temperature of an ideal Bose gas is proportional to $N_B^{2/3}$ (where N_B is the number of bosons), T_c in the extreme BEC limit is given by

$$T_c = T_c^{\text{BEC}} \times \left[\frac{N_{\uparrow}}{(N/2)} \right]^{2/3} = T_c^{\text{BEC}} (1 - P)^{2/3}, \quad (17)$$

where $T_c^{\text{BEC}} = 0.218\varepsilon_F$ is T_c in the BEC limit of a unpolarized Fermi gas. $P = (N_{\uparrow} - N_{\downarrow})/(N_{\uparrow} + N_{\downarrow})$ is the polarization rate. Equation (17) indicates that T_c decreases with increasing P to vanish in the fully polarized limit ($P \rightarrow 1$).

In the crossover region, as well as the BCS regime, Fig.7 shows that T_c vanishes at a certain value of P ($\equiv P_c < 1$). Since a polarized Fermi gas in the BCS regime is similar to metallic superconductivity under an external magnetic field, the vanishing T_c at P_c (< 1) is essentially the same as the suppression of the superconducting state by an external magnetic field. In the unitarity limit, one finds $P_c = 0.13$, which is relatively close to the observed polarization rate $P_{tc} = 0.2$ at the tricritical point of a ${}^6\text{Li}$ Fermi gas [58, 59].

In the mean-field theory, the region of the phase separation (PS), which is surrounded by the first-order phase transition line, is obtained in the $T - P$ phase diagram, as shown in Fig.8. (We summarize how to obtain this figure in Appendix B.) Since the mean-field theory is valid for the weak-coupling regime, the PS region would also appear in Fig.7, if one included the possibility of the first-order phase transition beyond the present treatment. To confirm this, however, we need to evaluate the thermodynamic potential Ω , taking into account strong-coupling corrections within the framework of ETMA, which remains as our future problem.

Figure 9(a) shows effects of the “effective magnetic field” h on the superfluid phase transition. As expected from the magnetic field effect on superconductivity, T_c decreases with increasing h to vanish at a critical magnetic field h_c . When we evaluate the polarization rate P along this T_c -line, we obtain Fig.9(b). In this panel, T_c is almost constant around $h = 0$, $(dP/dh)_{h \rightarrow 0}$ is close to the spin susceptibility χ (> 0). Thus, in a sense, the positive

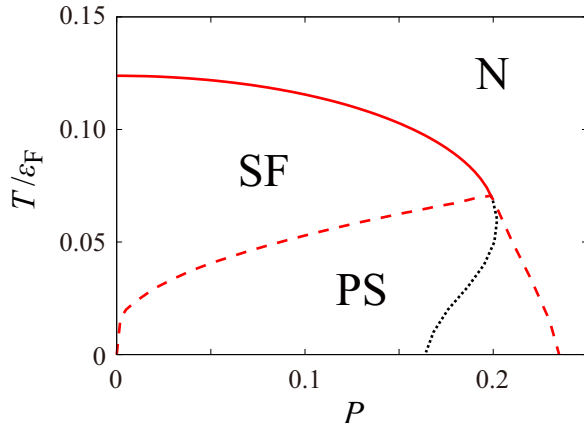


FIG. 8: (color online) Mean-field phase diagram of a polarized Fermi gas when $(k_F a_s)^{-1} = -1$. The solid line shows the second-order phase transition between the superfluid phase (SF) and the normal state (N). The dashed line shows the first-order phase transition, below which the phase separation (PS) of the superfluid phase and the normal state occurs. The tricritical point is obtained at $P_{tc} = 0.199$. When we ignore the PS phase and simply assume the second-order superfluid phase transition, we obtain the dotted line. In this case, one finds $P_c = 0.202$. Assuming the second-order phase transition (solid line and dotted line), the reentrant region is obtained when $0.164 \leq P \leq 0.202 (= P_c)$.

P in panel (b) is a result of the correct treatment of the spin susceptibility in ETMA.

In the inset of Fig.9(b), one sees a peak structure near the critical magnetic field h_c . Since P_c is given by this peak value, P_c is found to obtain, not at h_c , but below h_c . As expected from the mean-field phase diagram shown in Fig.8, one needs a more sophisticated treatment near P_c and h_c to include the first-order phase transition, as well as phase separation. However, apart from this, the origin of the peak seen in the inset of Fig.9(b) is explained as follows. When the temperature T is fixed at a certain value, P monotonically increases with increasing h . On the other hand, when one decreases the temperature under the condition of a fixed h , the polarization P may decrease near T_c , because of the suppression of the spin susceptibility due to the development of the pseudogap. (See Fig.6.) In the case of Fig.9, because the both mechanisms affect P , the polarization rate may decrease, when the latter effect becomes dominant. In particular, since the decreases of T_c is most remarkable near h_c (See Fig.9(a).), this remarkable decrease of the temperature leads to the decrease of χ ,

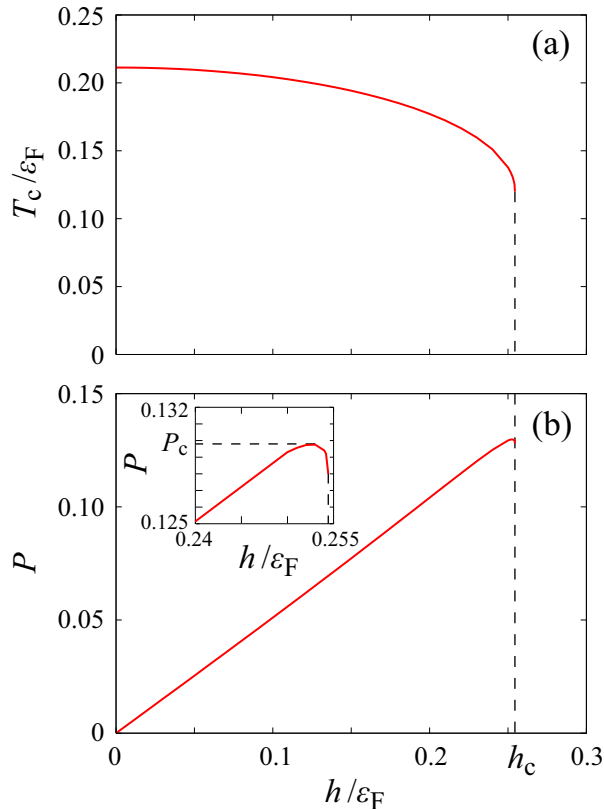


FIG. 9: (color online) (a) Calculated T_c , as a function of the “effective magnetic field” h . We take $(k_F a_s)^{-1} = 0$. (b) Polarization rate P at T_c , as a function of h . The inset shows the polarization near the critical magnetic field h_c at which the second-order phase transition disappears. The critical polarization rate P_c is determined as the peak value seen in the inset.

as well as P , as shown in the inset of Fig.9(b). We briefly note that, since the temperature is not fixed in panel (b), the negative value of $(dP/dh)_{h \simeq h_c}$ does not mean the violation of the required positivity of the spin susceptibility. In ETMA, the spin susceptibility is always positive, when the temperature is fixed.

V. SUMMARY

To summarize, we have investigated magnetic properties of a cold Fermi gas in the BCS-BEC crossover region. In the NSR theory, it is known that the spin susceptibility becomes negative in the crossover region. We showed that this unphysical result is also obtained in the ordinary (non-self-consistent) T -matrix approximation. We clarified that this negative

spin susceptibility originates from how to treat the self-energy correction and vertex correction to the spin susceptibility. Improving this, we have succeeded in obtaining the positive spin susceptibility over the entire BCS-BEC crossover region. The calculated spin susceptibility agrees well with the recent experiment done by Sanner and co-workers [47], without introducing any fitting parameter. We have also applied our extended T -matrix theory to a polarized Fermi gas, and have calculated T_c in the BCS-BEC crossover region.

In this paper, we have considered the normal state above T_c . Since the spin susceptibility is known to be strongly suppressed in the superfluid phase below T_c , it is an interesting next challenge to extend the present theory to include the superfluid order parameter. This extension is also necessary in considering the first-order phase transition, as well as the phase separation, expected in polarized Fermi superfluids.

In addition, we have only treated a uniform gas, for simplicity. Since a real cold Fermi gas is always trapped in a harmonic potential, the inclusion of this spatial inhomogeneity is crucial for detailed comparison of theoretical results with experimental data. However, since the key issues to overcome the negative susceptibility problem clarified in this paper is also valid for a trapped gas, our results would be useful for the further development of research for magnetic properties of trapped polarized Fermi gases.

Acknowledgements

We would like to thank S. Watabe, Y. Endo, D. Inotani, and R. Hanai for useful discussions. Y. O. was supported by Grant-in-Aid for Scientific research from MEXT in Japan (No.22540412, No.23104723, No.23500056).

Appendix A: Derivation of Eq. (13)

In the NSR theory, strong-coupling correction ($\equiv \chi_{\text{NSR}}^{\text{fluct}}$) to the spin susceptibility with $O(\Sigma^0)$ is given by

$$\chi_{\text{NSR}}^{\text{fluc}} = \frac{\partial}{\partial h} \left[T \sum_{\mathbf{p}, i\omega_n, \sigma} \sigma G_{\mathbf{p}, \sigma}^0(i\omega_n) \Sigma_{\mathbf{p}, \sigma}^0(i\omega_n) G_{\mathbf{p}, \sigma}^0(i\omega_n) \right]_{h \rightarrow 0}. \quad (\text{A1})$$

Carrying out the h -derivative, we obtain the contributions in Figs.4(b2) and (b3). Their expressions are given by, respectively,

$$\begin{aligned}\chi_{\text{NSR}}^{(\text{b2})} &= -2T \sum_{\mathbf{p}, i\omega_n, \sigma} [G_{\mathbf{p}, \sigma}^0(i\omega_n)]^3 \Sigma_{\mathbf{p}, \sigma}^0(i\omega_n) \Big|_{h=0} \\ &= -T \sum_{\mathbf{q}, i\nu_n, \sigma} \Gamma(\mathbf{q}, i\nu_n) \frac{\partial^2}{\partial \mu_\sigma^2} \Pi(\mathbf{q}, i\nu_n) \Big|_{h=0},\end{aligned}\quad (\text{A2})$$

$$\begin{aligned}\chi_{\text{NSR}}^{(\text{b3})} &= 2T^2 \sum_{\mathbf{p}, i\omega_n} \sum_{\mathbf{q}, i\nu_n} \Gamma(\mathbf{q}, i\nu_n) [G_{\mathbf{p}, \uparrow}^0(i\omega_n)]^2 [G_{\mathbf{q}-\mathbf{p}, \downarrow}^0(i\nu_n - i\omega_n)]^2 \Big|_{h=0} \\ &= 2T \sum_{\mathbf{q}, i\nu_n} \Gamma(\mathbf{q}, i\nu_n) \frac{\partial^2}{\partial \mu_\uparrow \partial \mu_\downarrow} \Pi(\mathbf{q}, i\nu_n) \Big|_{h=0}.\end{aligned}\quad (\text{A3})$$

In the BEC limit, the particle-particle vertex function in Eq. (7) reduces to [60],

$$\Gamma(\mathbf{q}, i\nu_n) \simeq \frac{8\pi}{m^2 a_s} \frac{1}{i\nu_n - \frac{q^2}{4m} + \mu_B}.\quad (\text{A4})$$

Here, $\mu_B = 2\mu + \epsilon_b$ may be regarded as the chemical potential of molecular bosons, where $\epsilon_b = 1/ma_s^2$ is the binding energy of a two-body bound molecule. Using the fact that the binding energy ϵ_b is very large in the BEC limit ($a_s^{-1} \rightarrow \infty$), one may expand $\partial^2 \Pi(\mathbf{q}, i\nu_n) / \partial \mu_\uparrow^2$ in Eq. (A2) with respect to ϵ_b^{-1} . We then have

$$\begin{aligned}\frac{\partial^2}{\partial \mu_\uparrow^2} \Pi(\mathbf{q}, i\nu_n) &= \sum_{\mathbf{p}} \frac{1}{i\nu_n - \xi_{\mathbf{p}+\mathbf{q}/2, \uparrow} - \xi_{\mathbf{p}-\mathbf{q}/2, \downarrow}} \frac{\partial^2 f(\xi_{\mathbf{p}+\mathbf{q}/2, \uparrow})}{\partial \mu_\uparrow^2} + O(\epsilon_b^{-2}) \\ &\simeq -\frac{1}{\epsilon_b} \frac{\partial^2 N_\uparrow^0}{\partial \mu_\uparrow^2} + O(\epsilon_b^{-2}),\end{aligned}\quad (\text{A5})$$

where $N_\uparrow^0 = \sum_{\mathbf{p}} f(\xi_{\mathbf{p}, \uparrow})$ is the number of \uparrow -spin atoms in a free Fermi gas. Substituting Eq. (A5) into Eq. (A2), one obtains

$$\chi_{\text{NSR}}^{(\text{b2})} = \frac{2T}{\epsilon_b} \frac{\partial^2 N_\uparrow^0}{\partial h^2} \Big|_{h=0} \sum_{\mathbf{q}, i\nu_n} \Gamma(\mathbf{q}, i\nu_n).\quad (\text{A6})$$

In particular, at T_c , we find

$$\chi_{\text{NSR}}^{(\text{b2})} = -\frac{16\pi a_s}{m} \left(\frac{2mT_c}{2\pi} \right)^{\frac{3}{2}} \zeta \left(\frac{3}{2} \right) \frac{\partial^2 N_\uparrow^0}{\partial h^2} \Big|_{h=0}.\quad (\text{A7})$$

We briefly note that, because $\partial^2 \Pi(\mathbf{q}, i\nu_n) / \partial \mu_\uparrow \partial \mu_\downarrow$ is the order of ϵ_b^{-2} , one finds $\chi_{\text{NSR}}^{(\text{b3})} = O(\epsilon_b^{-2})$. Thus, one can ignore $\chi_{\text{NSR}}^{(\text{b3})}$ in the BEC regime.

Appendix B: Mean-field phase diagram of a polarized Fermi gas

In the mean-field theory, the second-order phase transition is determined by solving the ordinary BCS gap equation at T_c ,

$$1 = U \sum_{\mathbf{p}} \frac{1 - f(\xi_{\mathbf{p},\uparrow}) - f(\xi_{\mathbf{p},\downarrow})}{\xi_{\mathbf{p},\uparrow} + \xi_{\mathbf{p},\downarrow}}, \quad (\text{B1})$$

together with the number equation,

$$N = \sum_{\mathbf{p},\sigma} f(\xi_{\mathbf{p},\sigma}). \quad (\text{B2})$$

To evaluate the first-order phase transition temperature, we need to consider the thermodynamic potential Ω in the presence of phase separation (PS), which is given by

$$\Omega(\mu_{\uparrow}, \mu_{\downarrow}, T, \Delta, x) = x\Omega_{\text{SF}}(\mu_{\uparrow}, \mu_{\downarrow}, T, \Delta) + (1-x)\Omega_{\text{N}}(\mu_{\uparrow}, \mu_{\downarrow}, T). \quad (\text{B3})$$

Here, Ω_{SF} and Ω_{N} are the thermodynamic potential in the superfluid (SF) phase and the normal state (N) region, respectively. Their mean-field expressions are given by

$$\Omega_{\text{SF}} = -\frac{m\Delta^2}{4\pi a_s} + \sum_{\mathbf{p}} \left[\xi_{\mathbf{p},\downarrow} - E_{\mathbf{p},\downarrow} + \frac{\Delta^2}{2\epsilon_{\mathbf{p}}} \right] - T \sum_{\mathbf{p},\sigma} \log(1 + e^{-E_{\mathbf{p},\sigma}/T}), \quad (\text{B4})$$

$$\Omega_{\text{N}} = -T \sum_{\mathbf{p},\sigma} \log(1 + e^{-\xi_{\mathbf{p},\sigma}/T}), \quad (\text{B5})$$

where $E_{\mathbf{p},\sigma} = \sqrt{\xi_{\mathbf{p}}^2 + \Delta^2} - \sigma h$ is the Bogoliubov excitation energy. Since any intensive variable should have the same value in both the SF region and the N region in the PS phase, each of the chemical potential μ_{σ} and the temperature T takes the same value in Ω_{SF} and Ω_{N} . The superfluid order parameter Δ and the volume fraction x of the SF region are, respectively, determined from the stationary conditions of Ω ,

$$0 = \frac{\partial \Omega}{\partial \Delta} = \frac{\partial \Omega_{\text{SF}}}{\partial \Delta}, \quad (\text{B6})$$

$$0 = \frac{\partial \Omega}{\partial x} = \Omega_{\text{SF}} - \Omega_{\text{N}}. \quad (\text{B7})$$

Equation (B6) gives the ordinary mean-field BCS gap equation. Equation (B7) simply means $\Omega_{\text{SF}} = \Omega_{\text{N}}$. We solve Eqs. (B6) and (B7), together with the number equations,

$$N_{\uparrow} = xN_{\uparrow,\text{SF}}(\mu_{\uparrow}, \mu_{\downarrow}, \Delta) + (1-x)N_{\uparrow,\text{N}}(\mu_{\uparrow}, \mu_{\downarrow}), \quad (\text{B8})$$

$$N_{\downarrow} = xN_{\downarrow,\text{SF}}(\mu_{\uparrow}, \mu_{\downarrow}, \Delta) + (1-x)N_{\downarrow,\text{N}}(\mu_{\uparrow}, \mu_{\downarrow}), \quad (\text{B9})$$

to self-consistently determine Δ , x , μ_σ , below T_c . In Eqs. (B8) and (B9), $N_{\sigma,\text{SF}}$ and $N_{\sigma,\text{N}}$ are the number of σ -spin atoms in the superfluid region and the normal state region, respectively.

The phase transition temperature T_c from the PS phase to the normal state is obtained as the temperature at which the superfluid volume fraction x vanishes ($x = 0$). The phase boundary between the PS phase and the superfluid phase is determined by the condition $x = 1$. We have numerically evaluated these conditions to obtain the phase diagram in Fig. 8.

-
- [1] L. D. Landau and E. M. Lifshitz, *Statistical Physics* (Pergamon, Oxford, 1980), Vol. 1, Chap. 5.
 - [2] A. A. Abrikosov, *Fundamentals of the Theory of Metals* (North-Holland, Amsterdam, 1988), Chap. 21.
 - [3] H. Yasuoka, T. Imai, and T. Shimizu, in *Strong Correlation and Superconductivity*, edited by H. Fukuyama, S. Maekawa, and A. P. Malozemoff (Springer Verlag, Berlin, 1989), p. 254.
 - [4] M. Randeria, in *Proceedings of the International School of Physics "Enrico Fermi" Course CXXXVI on High Temperature Superconductors*, edited by G. Iadonisi, J. R. Schrieffer, and M. L. Chialfalo, (IOS Press, Amsterdam, 1998), p. 53.
 - [5] C. A. Regal, M. Greiner, and D. S. Jin, *Phys. Rev. Lett.* **92**, 040403 (2004).
 - [6] M. W. Zwierlein, C. A. Stan, C. H. Schunck, S. M. F. Raupach, A. J. Kerman, and W. Ketterle, *Phys. Rev. Lett.* **92**, 120403 (2004).
 - [7] J. Kinast, S. L. Hemmer, M. E. Gehm, A. Turlapov, and J. E. Thomas, *Phys. Rev. Lett.* **92**, 150402 (2004).
 - [8] M. Bartenstein, A. Altmeyer, S. Riedl, S. Jochim, C. Chin, J. H. Denschlag, and R. Grimm, *Phys. Rev. Lett.* **92**, 203201 (2004).
 - [9] S. Giorgini, L. Pitaevskii, and S. Stringari, *Rev. Mod. Phys.* **80**, 1215 (2008).
 - [10] I. Bloch, J. Dalibard, and W. Zwerger, *Rev. Mod. Phys.* **80**, 885 (2008).
 - [11] Q. J. Chen, J. Stajic, S. Tan, and K. Levin, *Phys. Rep.* **412**, 1 (2005).
 - [12] C. Chin, R. Grimm, P. Julienne, and E. Tiesinga, *Rev. Mod. Phys.* **82**, 1225 (2010).
 - [13] D. M. Eagles, *Phys. Rev.* **186**, 456 (1969).
 - [14] A. J. Leggett, in *Modern Trends in the Theory of Condensed Matter*, edited by A. Pekalski

- and J. Przystawa (Springer Verlag, Berlin, 1980), p. 14.
- [15] P. Nozières and S. Schmitt-Rink, *J. Low Temp. Phys.* **59**, 195 (1985).
 - [16] C. A. R. Sa de Melo, M. Randeria, and J. R. Engelbrecht, *Phys. Rev. Lett.* **71**, 3202 (1993).
 - [17] Y. Ohashi and A. Griffin, *Phys. Rev. Lett.* **89**, 130402 (2002).
 - [18] J. T. Stewart, J. P. Gaebler, and D. S. Jin, *Nature* **454**, 744 (2008).
 - [19] J. P. Gaebler, J. T. Stewart, T. E. Drake, D. S. Jin, A. Perali, P. Pieri, and G. C. Strinati, *Nature Physics*, **6**, 569 (2010).
 - [20] S. Tsuchiya, R. Watanabe, and Y. Ohashi, *Phys. Rev. A* **80**, 033613 (2009); *ibid.*, **82**, 033629 (2010); *ibid.*, **84**, 043647 (2011).
 - [21] Q. Chen and K. Levin, *Phys. Rev. Lett.* **102**, 190402 (2009).
 - [22] P. Magierski, G. Wlazlowski, A. Bulgac, and J. E. Drut, *Phys. Rev. Lett.* **103**, 210403 (2009).
 - [23] R. Watanabe, S. Tsuchiya, and Y. Ohashi, *Phys. Rev. A* **82**, 043630 (2010); *ibid.*, **85** 039908 (2012).
 - [24] H. Hu, X.-J. Liu, P. D. Drummond, and H. Dong, *Phys. Rev. Lett.* **104**, 240407 (2010).
 - [25] S.-Q. Su, D. E. Sheehy, J. Moreno, and M. Jarrell, *Phys. Rev. A* **81**, 051604(R) (2010).
 - [26] A. Perali, F. Palestini, P. Pieri, G. C. Strinati, J. T. Stewart, J. P. Gaebler, T. E. Drake, and D. S. Jin, *Phys. Rev. Lett.* **106**, 060402 (2011).
 - [27] E. J. Mueller, *Phys. Rev. A* **83**, 053623 (2011).
 - [28] M. W. Zwierlein, A. Schirotzek, C. H. Schunck, and W. Ketterle, *Science* **311**, 492 (2006).
 - [29] G. B. Partridge, W. Li, R. I. Kamar, Y.-A. Liao, and R. G. Hulet, *Science* **311**, 503 (2006).
 - [30] A. M. Clogston, *Phys. Rev. Lett.* **9** 266 (1962).
 - [31] P. Fulde and R. A. Ferrell, *Phys. Rev.* **135**, A550 (1964).
 - [32] A. I. Larkin and Y. N. Ovchinnikov, *Sov. Phys. JETP* **20**, 762 (1965).
 - [33] G. Sarma, *J. Phys. Chem. Solids* **24**, 1029 (1963).
 - [34] W. V. Liu and F. Wilczek, *Phys. Rev. Lett.* **90**, 047002 (2003).
 - [35] For a review, see D. E. Sheehy and L. Radzihovsky, *Ann. Phys. (N.Y.)* **322**, 1790 (2007).
 - [36] P. Pieri and G. C. Strinati, *Phys. Rev. B* **61**, 15370 (2000).
 - [37] J. N. Milstein, S. J. J. M. F. Kokkelmans, and M. J. Holland, *Phys. Rev. A* **66**, 043604 (2002).
 - [38] Y. Ohashi and A. Griffin, *Phys. Rev. A* **67**, 033603 (2003).
 - [39] J. Stajic, J. N. Milstein, Q. Chen, M. L. Chiofalo, M. J. Holland, and K. Levin, *Phys. Rev. A* **69**, 063610 (2004).

- [40] H. Hu, X.-J. Liu, and P. D. Drummond, *Europhys. Lett.* **74** 574, (2006).
- [41] R. B. Diener, R. Sensarma, and M. Randeria, *Phys. Rev. A* **77**, 023626 (2008).
- [42] X.-J. Liu and H. Hu, *Europhys. Lett.* **75**, 364 (2006).
- [43] M. M. Parish, F. M. Marchetti, A. Lamacraft, and B. D. Simons, *Nat. Phys.* **3**, 124 (2007).
- [44] G. L. Sewell, *Quantum Mechanics and its Emergent Macrophysics* (Princeton University Press, Princeton, NJ, 2002).
- [45] H. Shimahara, *J. Phys. Soc. Jpn.* **67** 1872 (1998).
- [46] Y. Ohashi, *J. Phys. Soc. Jpn.* **71**, 2625 (2002).
- [47] C. Sanner, E. J. Su, A. Keshet, W. Huang, J. Gillen, R. Gommers, and W. Ketterle, *Phys. Rev. Lett.* **106**, 010402 (2011).
- [48] We note that ETMA still uses the bare Green's functions in the particle-particle scattering vertex Γ . When the full Green's functions are also used in Γ , we obtain the self-consistent T -matrix theory.
- [49] For example, the spin susceptibility χ_0 of a free Fermi gas at $T = 0$ is given by $\chi_0 = 2\rho(0)$.
- [50] A. A. Varlamov, G. Balestrino, E. Milani, and D. V. Livanov, *Adv. Phys.* **48**, 655 (1999).
- [51] We note that the so-called Aslamazov-Larkin type diagrams vanish identically in the spin susceptibility.
- [52] The last term in Fig.4(b) also has the same physical meaning as $-U\bar{\chi}_0^2$ appearing in TMA.
- [53] A. Sommer, M. Ku, G. Roati, and M. W. Zwierlein, *Nature (London)* **472**, 201 (2011).
- [54] Y. Yoshinari, H. Yasuoka, Y. Ueda, K. Koga, and K. Kosuge, *J. Phys. Soc. Jpn.* **59**, 3698 (1990).
- [55] E. Taylor, S. Zhang, W. Schneider, and M. Randeria, *Phys. Rev. A* **84**, 063622 (2011).
- [56] F. Palestini, P. Pieri, and G. C. Strinati, *Phys. Rev. Lett.* **108**, 080401 (2012).
- [57] In the BCS region, as well as the crossover region, one obtains a reentrant behavior of T_c near P_c , where two T_c' are obtained for a given P . This phenomenon can be also seen in the mean-field phase diagram in Fig.9, when the second-order phase transition is assumed. However, Fig.9 indicates that the first-order phase transition accompanied by the phase separation cannot be ignored near P_c , so that a more sophisticated treatment would be necessary in determining the phase diagram around the reentrant region near P_c . In Fig.8, we only plot the higher T_c in the reentrant region, and set $T_c = 0$ when $P > P_c$.
- [58] Y. Shin, C. H. Schunck, A. Schirotzek, and W. Ketterle, *Nature* **451**, 689 (2008).

- [59] At the tricritical point P_{tc} , the superfluid phase transition changes from the second-order type to the first-order type. Although the present calculation ignores the first-order phase transition, the value of P_{tc} is expected to be close to P_c determined as the largest value of P where the second-order phase transition occurs. Indeed, in the mean-field phase diagram shown in Fig.8, one finds that $P_{tc} = 0.199$, and $P_c = 0.202$.
- [60] R. Hausmann, Z. Phys. B **91**, 291 (1993).